Saberi and Harvey *Fire Ecology* (2023) 19:24
https://doi.org/10.1186/s42408-023-00178-3

Fire Ecology

ORIGINAL RESEARCH

Open Access

What is the color when black is burned? Quantifying (re)burn severity using field and satellite remote sensing indices

Saba J. Saberi[1*] and Brian J. Harvey[1]

Abstract

Background Trends of increasing area burned in many regions worldwide are leading to more locations experiencing short-interval reburns (i.e., fires occurring two or more times in the same place within 1–3 decades). Field and satellite indices of burn severity are well tested in forests experiencing a single recent fire, but the reliability of these indices in short-interval reburns is poorly understood. We tested how a commonly used field index (the Composite Burn Index, CBI) and satellite index (the Relative differenced Normalized Burn Ratio, RdNBR) compared to eight individual field measures of burn severity in short-interval reburns vs. areas burned in one recent fire, and whether results depended on whether the first fire was stand replacing (fire that is lethal to most dominant trees).

Results Correspondence between both CBI and RdNBR with individual burn severity measures differed in short-interval reburns compared to single fires for some metrics of burn severity. Divergence in the relationship between both CBI and RdNBR vs. field measures was greatest when short-interval reburns followed a prior stand-replacing fire, and measures were more comparable to single fires when the first fire was non-stand replacing (i.e., lower severity). When short-interval reburns followed prior stand-replacing fires, CBI and RdNBR underestimated burn severity in the second fire for tree-canopy metrics (e.g., canopy cover loss, tree mortality), as young forests in early developmental stages are more sensitive to a second fire. Conversely, when short-interval reburns followed prior less-than-stand-replacing fires, both CBI and RdNBR overestimated burn severity for forest-floor metrics, as past low severity fires leave behind live fire-resistant trees and can stimulate resprouting understory vegetation. Finally, neither CBI nor RdNBR accurately detected deep wood charring—an important phenomenon that occurs in short-interval reburns.

Conclusion Our findings inform interpretability of commonly used indices of burn severity in short-interval reburns by identifying how individual burn severity metrics can be under- or over-estimated, depending on the severity of the fire preceding a reburn. Adjustments to burn severity measurements made in short-interval reburns are particularly critical as reburned areas increase.

Keywords CBI, RdNBR, Wildfire, Disturbance interactions, Reburns, Stand-replacing fire, Extreme burn severity

*Correspondence:
Saba J. Saberi
sjsaberi@ucdavis.edu
[1] School of Environmental and Forest Sciences, University of Washington, Seattle, WA, USA

Resumen

Antecedentes La tendencia en la aceleración de áreas quemadas en forma en varias regiones del planeta está llevando a incrementos en la cantidad de áreas que experimentan intervalos de quema cortos (por ej. fuegos ocurridos dos o más veces en el mismo lugar en 1 a 3 décadas). Índices de severidad de las quemas de campo y de satélite han sido muy bien probados en bosques que experimentaron un solo fuego reciente, pero la confiabilidad de estos índices en intervalos cortos de luego de una segunda quema no está muy bien entendida. Probamos un índice de campo (el Composite Burn Index, CBI) e índices satelitales (la diferencia relativa de la tasa de quema normalizada, RdNBR) comparada con ocho medidas de campo individuales en áreas quemadas varias veces vs. áreas quemadas una sola vez y recientemente. También probamos si las relaciones en las áreas quemadas dos veces dependieron de que el primer fuego fuera uno de reemplazo del rodal (fuego letal para la mayoría de los árboles dominantes).

Resultados La correspondencia entre ambas CBI y RdNBR con medidas individuales de severidad de fuego difirieron entre las áreas quemadas por segunda vez comparadas con áreas quemadas por fuegos individuales para algunas medidas de severidad del fuego. La divergencia en la relación entre ambos CBI y RdNBR vs. las medidas de campo fue mayor cuando las quemas repetidas ocurrieron luego de un fuego de reemplazo del rodal, y las medidas fueron más comparables a fuegos individuales cuando el primer fuego no fue de reemplazo (de baja intensidad). Cuando los sitios quemados dos veces ocurrieron donde el fuego precedente fue de reemplazo, CBI y RdNBR subestimaron la severidad de la quema en el segundo fuego para medidas del canopeo de los árboles (por ej. pérdida de la cobertura del canopeo y mortalidad de los árboles), ya que bosques post-fuego en estados tempranos de desarrollo son vulnerables a segundos fuegos de mayor severidad. En cambio, cuando las segundas quemas sucedieron a un fuego precedente que no fue de reemplazo del rodal, ambos CBI y RdNBR sobrestimaron la severidad de la superficie quemada, ya que los fuegos pasados de baja severidad dejan árboles vivos que resisten al fuego y pueden estimular el rebrote de la vegetación debajo del dosel. Finalmente, ni el CBI ni el RdNBR fueron capaces de detectar en forma precisa la cantidad de madera carbonizada en la profundidad del tronco que ha emergido como un producto importante en las segundas quemas –particularmente en donde ambos fuegos son de reemplazo del rodal.

Conclusiones Nuestros hallazgos informan la interpretabilidad de los índices comúnmente utilizados en la severidad de las quemas y sequndas quemas, lo cual se está convirtiendo en una aplicación cada vez más común a medida que la actividad del fuego se incrementa.

The sky is blue and so is the sea. What is the color when black is burned? (Neil Young, “I am a child”, 1979)

Introduction

Increasing area burned in forested regions around the world is leading to many areas burning more than once in short-interval reburns (areas that have experienced two fires within 1–3 decades, Prichard et al. 2017). Reburns are expected in any fire-prone region, as fires have historically recurred at some interval characteristic of the fire regime. However, the ecological consequences of contemporary short-interval reburns can differ based on context, and areas affected by short-interval reburns have received heightened attention in recent decades. For example, in forests adapted to historically frequent fire, short-interval reburns can represent a return to historical fire-return intervals and foster resilience to fire by reducing fuel loads (Stevens-Rumann and Morgan 2016) and favoring thick-barked fire-resistant trees (Larson et al. 2013). In contrast, in forests with historically longer fire-return intervals, short-interval reburns can overwhelm resilience mechanisms (e.g., time required for seed production sufficient for post-fire forest regeneration, Enright et al. 2015), and produce novel extreme levels of burn severity that erode biological legacies (Donato et al. 2009b, 2016; Turner et al. 2019). Building an understanding of how to quantify burn severity in short-interval reburns and accurately tracking trends in such metrics is therefore important for characterizing changing fire regimes and their ecological impacts.

Reliable and widely used indices exist to measure burn severity in the field or remotely with earth-observing satellites, and many models have been developed to link field- and satellite data for widespread mapping of fire effects. The Composite Burn Index (CBI) is a unitless semi-quantitative index of burn severity produced via ocular estimation of fire effects across five forest strata in a 30-m diameter field plot. CBI is widely used as a standard post-fire assessment, though it was developed primarily to validate satellite remote-sensing indices (Key and Benson 2006). CBI values are scaled from zero to three, with zero representing an unburned area and three representing a severely burned area with complete vegetation mortality. Although CBI values can be resolved to whatever precision a user desires (e.g., plot-level averages to 1–2 decimal points), they are commonly collapsed into categories of low (0.75–1.25), moderate-high (1.25–2.25), and high (2.25–3) severity (Fig. 1) for use in describing fire effects or calibrating satellite maps (Picotte and Robertson 2011). CBI is useful in that it is a relatively quick (requiring less than one hour per plot) field protocol which corresponds well with field measures based on plant injury, fuel consumption, and tree mortality (Miller et al. 2009). Individual field measures such as fire-killed tree basal area and char height have also been established as additional metrics of burn severity (e.g., Harvey et al. 2014), and CBI generally corresponds well with many of these independently measured metrics (Saberi et al. 2022).

Satellite-derived burn severity indices are commonly based on the normalized burn ratio (NBR)—which uses the ratio of the difference between near infrared and shortwave infrared spectral bands from pre-and post-fire Landsat imagery to detect fire-caused vegetation changes (Key and Benson 2006). The differenced normalized burn ratio (dNBR), relative differenced normalized burn ratio (RdNBR, Miller and Thode 2007), and the relative burn ratio (RBR, Parks et al. 2014b) are widely used derivatives of the NBR and have been calibrated to CBI and other field measures (Cansler and McKenzie 2012). RdNBR was designed to better account for differences in pre-fire vegetation compared with dNBR, by further dividing by the square root of pre-fire NBR. This additional step of relativizing burn severity should be particularly useful in the context of short-interval reburns because it mitigates the effect of pre-fire vegetation on the possible range of severity values and is designed to help with comparisons among burned areas with different pre-fire starting points (Miller and Thode 2007). Finally, RdNBR is widely used among users of such indices to map fire effects (Huang et al. 2020; Konkathi and Shetty 2021). Despite the widespread use of these field and satellite indices to measure burn severity in both single burns and short-interval reburns (e.g., Parks et al. 2014a, Harvey et al. 2016a,b), how well they perform in short-interval reburns has not been widely tested.

A short-interval reburn could affect how these indices record burn severity in several ways. First, the severity (the magnitude of fire impacts on vegetation, Keeley 2009) of the first fire can affect forest structure in ways that lead to different vegetation present when a second fire occurs. For example, a first fire that is non-stand replacing (i.e., burns at low severity) is unlikely to drastically alter forest structure, leaving behind biological legacies such as live thick-barked, fire-resistant trees if they were present pre-fire. This is particularly common in low-severity and frequent-fire regimes dominated by trees with adaptations to survive low-intensity fires, and understory vegetation that can either re-sprout or regenerate quickly from seed (Agee 1996). Conversely, a first fire that is stand-replacing (high severity) produces greater effects on stand structure by killing trees, leaving fewer post-fire live biological legacies, and initiating secondary succession. This outcome is common in high-severity fire regimes dominated by trees with fewer adaptations to survive fire, but instead possessing adaptations such as aerial seedbanks or wind-dispersed seed (Agee 1996). When forests are in an early-seral stage due to a previous fire, short-interval reburns result in a second fire encountering young fire-sensitive tree seedlings and saplings with tree crowns close to the forest floor. In such

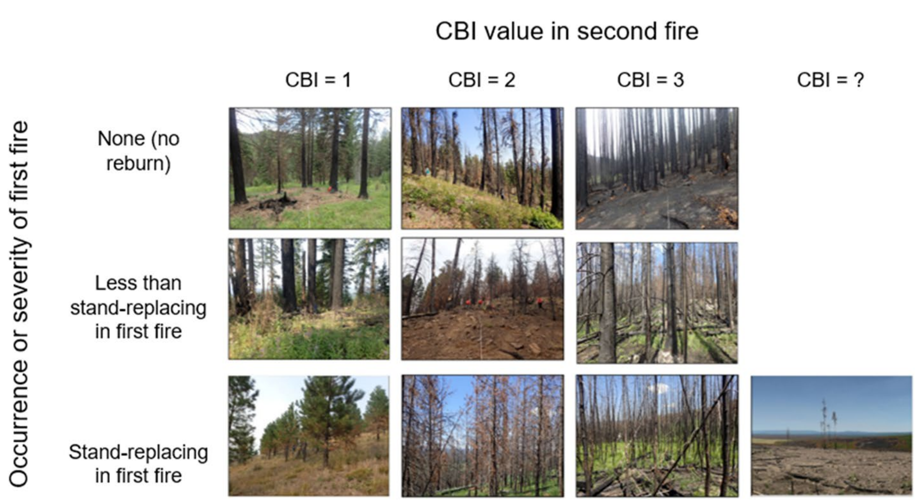

Fig. 1 Photos of burn severity in plots across differing severities of a previous burn

cases, burn severity in the second fire can be so extreme that most above-ground live, and downed woody material is consumed (e.g., Donato et al. 2009b, 2016, Turner et al. 2019, Fig. 1, bottom right panel). One important aspect of extreme burn severity in short-interval reburns can be the production of deep char, often the result of incomplete combustion of dead wood from extended periods of smoldering combustion (Donato et al. 2009b, Bird et al. 2015, Talucci and Krawchuk 2019). Deep char can be visually distinguished by its shiny, scaly appearance as opposed to the dusty and matte black appearance of scorch on a tree that was live prior to fire (Talucci and Krawchuk 2019), and has important ecological properties with regard to carbon storage, nutrient and water retention, and substrate quality (Pyne et al. 1996, Czimczick et al. 2002, Bradbury 2006, Maranon-Jimenez et al. 2013, Singh et al. 2012).Thus, it is possible that burn severity indices well-calibrated to single-fires may relate differently to burn severity in short-interval reburns depending on the severity of—and structural legacies left behind by—the first fire.

In this study, we address the above knowledge gaps by asking the following questions. First, how does the relationship between eight independent field measures of burn severity and CBI (Q1) and RdNBR (Q2) vary between single fires and areas that have experienced short-interval reburns? Further, in each question, we tested whether the relationship depended on if the first fire in a short-interval reburn was stand-replacing. We expect the relationships between individual field measures of burn severity and both CBI and RdNBR to differ depending on the severity of the previous fire and the magnitude of fire-caused changes to forest structure in the previous fire (i.e., biological legacies remaining after one fire). Additionally, for RdNBR, we expected differences to depend on the ability of the top-down perspective of the satellite sensor to capture spectral signatures from different forest strata or different stand densities. Finally, we asked how CBI or RdNBR capture indices of extreme burn severity (Q3) (e.g., deep charring and combustion of woody material) that has been observed in recent short-interval reburns (Turner et al. 2019).

Methods

Study area

The study area spans forested areas of the northwestern USA from the west side of the Cascade Mountains to the US Northern Rockies, across five states in the western United States (ID, MT, OR, WA, WY). Sampled forests were conifer dominated, containing thick-barked, fire-resistant trees at lower elevations including Douglas-fir

Table 1 Location, elevation range, dominant tree species, and fire characteristics of the 14 sampled fires, seven of which were short-interval reburns. Three of the sample locations contained plots in areas that had been previously burned by two different fires. Dominant tree species reflect rank order of species containing the highest percent basal area across each fire, with the minimum threshold set at 20%

Fire that was sampled for this study (year)	*Location*	*Short-interval reburn*	*Previous fire (year)*	*Reburn interval*	*Total plots*	*Reburn plots*
Berry (2016)	Grand Teton NP, WY	Yes	Glade, Huck (2000, 1988)	16,28	27	27
Maple (2016)	Yellowstone NP, WY	Yes	Fork (1988)	28	10	10
Pioneer (2016)	Boise NF, ID	Yes	Smokey Creek (1989)	27	15	1
Rail (2016)	Malheur NF, OR	Yes	Monument Rock (1989)	27	23	7
Rock Creek (2016)	Okanogan-Wenatchee NF, WA			N/A	11	N/A
Jolly Mountain (2017)	Okanogan-Wenatchee NF, WA			N/A	12	N/A
Jones (2017)	Willamette NF, OR	Yes	Clark (2003)	14	28	11
Liberty (2017)	Flathead NF, MT	Yes	Jocko Lakes, Mineral-Primm (2007,2003)	10, 14	9	6
Lolo Peak (2017)	Lolo NF, MT			N/A	21	N/A
Meyers (2017)	Beaverhead-Deerlodge NF, MT			N/A	24	N/A
Milli (2017)	Deschutes NF, OR	YES	Pole Creek, Cascade Crest (2012, 2006)	5, 11	65	21
Norse Peak (2017)	Baker-Snoqualmie NF, WA			N/A	35	N/A
Rebel (2017)	Willamette NF, OR			N/A	8	N/A
Rice Ridge (2017)	Flathead NF, MT			N/A	27	N/A
				TOTAL	315	83

Abbreviations: *NP* National Park, *NF* National Forest

(*Psuedotsuga menziesii*) Mirbel (Franco) and ponderosa pine (*Pinus ponderosa*) Douglas ex P. Lawson & C. Lawson, as well as thin-barked trees that recruit post-fire such as lodgepole pine (*Pinus contorta*) Douglas ex Loudon at higher elevations (Agee 1996). Other dominant species in our sample included: *Abies grandes* (Douglas ex D. Don) Lindl., *Abies lasiocarpa* Hook. (Nutt.), *Abies amabilis*, and *Tsuga heterophylla* (Raf.) Sarg. The study area spans wide gradients in elevation, moisture, and forest type, and included burned areas with both short-interval reburns and locations with longer (unknown) intervals since the prior fire (Table 1, see Saberi et al. 2022 for details).

Data collection

One-year post-fire burn severity field data were collected from within 14 fires across nine Nationals Forests and two National Parks in the Interior Pacific Northwest (Table 1) during the summers of 2017 and 2018. Seven of these fire perimeters were characterized as short-interval reburns, meaning that they had experienced more than one fire within the past 30 years as recorded in the Landsat satellite fire record (Table 1). Measures of burn severity recorded in the field included CBI and eight individual metrics.

Field sampling

Field site selection and methods are explained in detail in Saberi et al. (2022), and briefly described here. In each plot, we measured CBI and eight individual and independently quantified metrics of burn severity: change in live canopy cover, an index of needle retention, tree mortality (by basal area and number of trees), tree charring (height and circumference of tree bole), deep charring on the tree bole, and surface char on the forest floor (Table 2). Prior to field sampling, fire perimeters were identified as containing short-interval reburns by analyzing where past MTBS fires (dating back to 1984, the start date for MTBS-mapped fires) overlapped with the selected fire perimeters in ArcGIS 10.6.1, and sampling occurred within the reburn perimeters. In the field, trees were assessed to determine if they were live pre-fire (i.e., survived the previous fire if the plot was a reburn) or dead pre-fire (i.e., had been killed in the fire preceding the reburn), and each reburned plot was recorded as having an initial fire that was either stand-replacing or non-stand replacing. Field plot assignment by this category was cross-referenced for reburn plots with RdNBR maps of the first fire used to confirm the severity of the first fire as stand-replacing or non-stand-replacing.

Remote sensing indices

Fire perimeters were obtained from the USFS Geospatial Technology Applications Center (GTAC). We calculated each of three satellite indices (dNBR, RdNBR, and RBR) in Google Earth Engine using two methods as follows: (1) the mean composite method detailed in Parks et al. (2018) and (2) using single pre- and post- fire imagery as established by MTBS. For the single image method, pre-fire, and post-fire imagery for each of the 14 fires was obtained from the Landsat 8 Surface Reflectance Tier 1 Datasets from the Google Earth Engine satellite imagery catalog, at 30-m pixel resolution (Table A5). Dates for pre-fire and post-fire LANDSAT imagery were selected by finding the date of the highest NDVI value in the year prior to each fire. This was to account for the time of peak

Table 2 Description of Composite Burn Index (CBI) and all independent field measures of burn severity across all 315 plots. Note that all variables are ultimately in proportions ranging from 0–1

Variable Name	Variable description
CBI	Average CBI value per plot, converted to proportion from the 0 to 3 scale (e.g., CBI of 1.8 was converted to a proportion of 0.6 to scale accordingly with other metrics).
Change in live canopy cover	Average proportion change in live canopy cover per plot. Proportion of pre-fire canopy in burned plots was modeled using the relationship between plot basal area and proportion of live canopy in from unburned plots
Dead needle	Average needle index value per plot, averaged from 20 randomly selected trees alive at time of fire, converted to proportion from 0 to 7 scale (e.g., needle index of 3 = 0.43)
Killed BA	Proportion of average tree basal area alive at time of fire and killed by fire per plot
Killed trees	Proportion of average number of trees alive at time of fire killed by fire per plot
Char height	Average proportion of total tree height charred from 20 randomly selected dominant canopy trees alive at time of fire
Bole char	Average proportion of visible char on 20 randomly selected dominant canopy trees alive at time of fire
Deep char	Average deep char index value on 20 randomly selected dominant canopy trees alive at time of fire, converted to proportion from 0 to 2 scale
Surface char	Average proportion of plot containing charred material on surface, taken from 480 points every 10 cm apart along main plot axis (N–S, E–W)

'greenness' in each fire area. Date of maximum NDVI was calculated in GEE using the MODIS 250 m NDVI product. Pre- and post-fire Landsat imagery was selected from the GEE catalog by only considering images within three weeks of the anniversary date and with no cloud cover. We accounted for potential phenological differences between pre- and post-fire imagery by producing the dNBR offset value for each fire (Key and Benson 2006). The dNBR offset is useful when comparing burn severity among multiple fires, as the baseline spectral signature for green vegetation is set per fire. We determined the dNBR offset by calculating the mean dNBR value across all pixels located in a 180-m buffer around each fire perimeter (Parks et al. 2018), which quantifies dNBR differences among unburned pixels. The dNBR offset was subtracted from the original dNBR rasters, and the dNBR with the offset was used in calculation of RdNBR and RBR. Once dNBR, RdNBR, and RBR were calculated, raster values corresponding to each individual plot point were extracted using the extract function in the 'raster' package in R (version 3.4.3) via bilinear interpolation.

Comparison among the single-image and composite methods revealed no qualitative differences (summarized in "Results" section), and therefore proceeded with all further analyses using the mean composite method (Parks et al. 2018) as this method has become commonly adopted. We also compared the bivariate relationships between CBI, and the three satellite indices (dNBR, RdNBR, and RBR) to assess any differences before choosing one to proceed with further analyses. Performance was virtually indistinguishable, and therefore we used RdNBR as the satellite burn severity index for all subsequent analyses (summarized in "Results" section).

Data analysis

To test the correspondence of each field measure with CBI (Q1) or RdNBR (Q2) in short-interval reburns (as well as to test capacity to model deep char (Q3), we created zero-one inflated beta (ZOIB) (Ospina and Ferarri 2012) regression models with the quantitative field measure as the response variable and CBI or RdNBR as the predictor variable. ZOIB models are appropriate for proportional data that include 0, 1, and continuous proportions between 0 and 1, and combine aspects of logistic regression (which can model 0 and 1 but not proportions between) and beta regression (which can model proportions between 0 and 1, but not values = 0 or values = 1) (Ospina and Ferrari 2012). The ZOIB approach overcomes the challenges associated with using linear regression models that require transformation of the predictor or response variables and has been applied to similar analyses with burn severity data (Harvey et al. 2019; Saberi et al. 2022).

We applied ZOIB regression using general additive models, specifying zero/one beta inflated distributions to allow for 0 and 1 as values for the response variable using the "gamlss" package in R version 3.4.3 (see Saberi et al. 2022 for model details). For both model types, reburn levels were incorporated into the model structure. There were three reburn levels, indicating the presence and severity of the previous burn and were codified as follows: no reburn, non-stand replacing, and stand replacing. We used a strength of evidence approach by evaluating p-values at different levels (strong at $p < 0.01$ level, moderate at $< .05$, suggestive at $< .10$, Muff et al. 2022) for each factor level and interaction term would indicate if the intercept and/or slope for the model differs depending on the severity of the first burn. We adopted this approach to mitigate the exclusion of potentially meaningful ecological relationships in inherently noisy observational field data (Ramsey and Schafer 2012). We also developed models without the reburn interaction term and present those models for use in regionally calibrated general models of burn severity when short-interval reburns are unknown or not of concern. Originally, 315 field plots were sampled (233 no short-interval reburn, 33 reburn with non-stand-replacing first fire, and 49 reburn with stand-replacing first fire). Following established methods to trim the extreme tails of distributions in similar analyses (Lutz et al. 2011; Povak et al. 2020), we included 95% of the range of satellite index values (trimming the upper and lower 2.5% tails of the distribution for each index) prior to analyses. The resulting dataset retained 299 plots (221 no short-interval reburn, 32 reburn with non-stand-replacing first fire, and 46 reburn with stand-replacing first fire). The performance of each index using the full dataset and the dataset with trimmed tails of the distribution was compared in prior analyses (Saberi 2019), with no evidence for qualitative differences in either approach.

(See figure on next page.)

Fig. 2 Zero/one inflated beta regression models for each of the eight individual burn severity metrics with CBI as the predictor variable. In the first column, the no reburn shows model prediction values for non-reburns, while the reburn (1st fire not stand replacing) represents reburns where the first fire was non-stand replacing and the reburn (1st fire stand replacing) represents reburns where the first fire was stand replacing (**A**, **C**, **E**, **G**, **I**, **K**, **M**, **O**). The polygon around each line shows 95% confidence around mean predicted values from bootstrapping. Gray dots are the raw data points from the 299 sampled plots. The second column contains AUC values for each of the eight regression models across five thresholds of burn severity (which were created as dichotomization thresholds to produce ROC curves). Overall AUC values represent overall average across five thresholds (**B**, **D**, **F**, **H**, **J**, **L**, **N**, **P**)

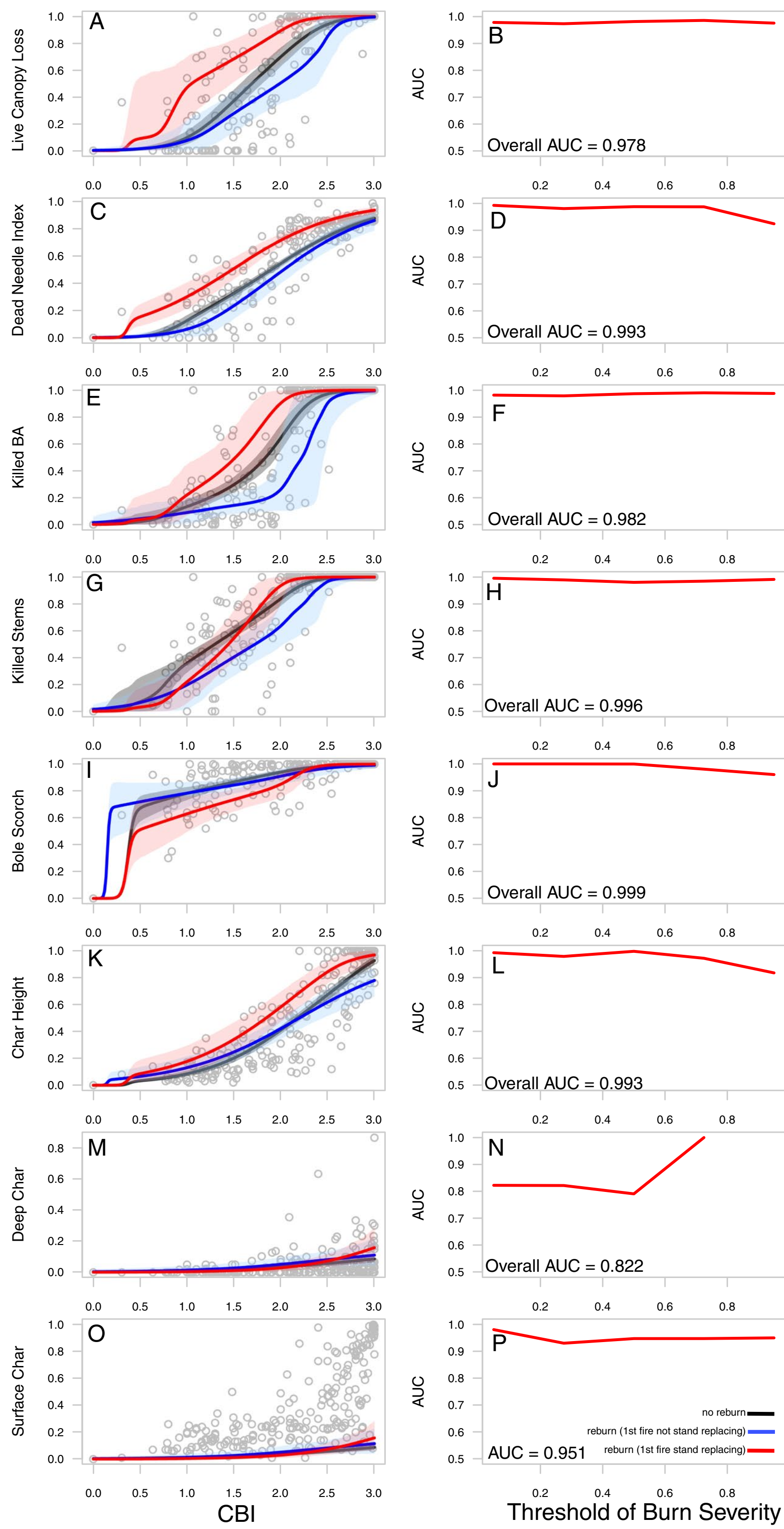

Fig. 2 (See legend on previous page.)

We evaluated model fit for all models using the area under receiver operating characteristic curves (AUC) for a sequence of proportion thresholds for the continuous field measure of burn severity (0.05.0.275, 0.5, 0.725, and 0.95). This approach allowed us to assess model fit across the burn severity gradient. AUC values were calculated by dichotomizing the field response proportions into zeroes and ones if they were above or below the given threshold values. As an AUC value below 0.5 indicates poor model fit/capacity to distinguish presence or absence, (Pearce and Ferrier 2000), we did not display values below this level.

Results

CBI and independent field measures in short-interval reburns (Q1)

The modeled relationship between CBI and independent field measures of burn severity in short-interval reburns was variable when compared to relationships in single fires, and divergence among models was generally greatest when the first fire was stand-replacing. When the first fire was stand-replacing, CBI in the second fire underestimated canopy cover change, needle loss, basal area (BA) killed by fire, and char height when compared to single burns (Fig. 2A, C, E, K). For example, a CBI score of 1.5 corresponded to canopy-cover change of approximately 25–35% in single fires or when short-interval fires followed non-stand-replacing fires but corresponded to canopy-cover change of approximately 60–80% when short-interval fires followed prior stand-replacing fires (Fig. 2A, difference between red line and black line). When the first fire was not stand-replacing, the primary difference between short-interval reburns and single burns was for surface char, where CBI overestimated surface char compared to single burns (Q1, Fig. 2O). For example, a CBI score of 2.5 corresponded to surface char of approximately 40–60% in single burns, but surface char of approximately 20% when short-interval fires followed non-stand-replacing fires (Fig. 2O, difference between blue line and black line). CBI did not correspond to deep charring on woody material (deep char) in short-interval reburns, regardless of the severity of the first fire (Q3, Fig. 2M, Tables A1 and A2). Model fit ranged from AUC 0.82 for deep char to AUC of 0.99 for tree mortality by basal area, tree mortality by number of trees, and bole scorch (Fig. 2F, H, L, Tables A1 and A2).

Satellite indices and field measures of burn severity in short-interval reburns (Q2)

No qualitative differences were detected in how satellite indices related to CBI between the mean composite method (mean AUC = 0.937) and the single pre-and post-fire image method (mean AUC = 0.942) (Fig. 3, Additional file 1: Tables S3-S7); therefore, all subsequent results are presented for the mean composite method given the standard adoption of this approach. Furthermore, we detected no qualitative differences among dNBR (AUC = 0.972), RdNBR (AUC = 0.986), and RBR (AUC = 0.973) in their correspondence to CBI (Fig. 3, Additional file 1: Tables A3, A4, A6, A7); therefore, all subsequent results are presented using RdNBR. RdNBR had strong correspondence to each of the eight individual field measures of burn severity overall (not accounting for reburns); we present these relationships for users who may be interested in using RdNBR outside of the context of reburns (Fig. 4, Additional file 1: Figure S1, Tables S8-S11).

The modeled relationship between RdNBR and field measures of burn severity was mostly similar between single fires and short-interval reburns when the first fire was non-stand-replacing; conversely, the relationship diverged more when short-interval reburns followed preceding stand-replacing fires (Q2, Fig. 5). When the first fire was stand-replacing, RdNBR in the second fire underestimated canopy cover loss, needle loss, BA killed by fire, and trees killed by fire, compared to single burns (Fig. 5C, E, G). For example, an RdNBR value of 400 corresponded to approximately 50% live canopy loss in single burns, but live canopy loss of approximately 90% when short-interval fires followed stand-replacing fires (Fig. 5C, difference between red line and black/blue lines). When the first fire was not stand-replacing, the only difference was for surface char, where RdNBR overestimated surface char compared to single burns (Fig. 5Q, Tables S12 and S13). For example, an RdNBR value of 800 corresponded to surface char of approximately 50% in single burns, but surface char of approximately 20% when short-interval fires followed non-stand-replacing fires (Fig. 3Q, difference between blue line and red/black lines). The RdNBR-based models had a high predictive ability for canopy measures, with the model for canopy cover, needle loss, killed basal area and killed trees producing an average AUC of 0.93, 0.95, 0.97 and 0.97, respectively across all burn severity

(See figure on next page.)

Fig. 3 Two panels comparing three zero/one inflated beta regression models with CBI as the response variable and dNBR, RdNBR, and RBR (calculated using the Parks et al. composite method on the left and with the single image paid method on the right) as the respective predictive variables. In the first column, the black line shows predicted response values. (**A**, **B**, **C**, **G**, **H**, **I**). The blue polygon around the line shows 95% confidence around mean predicted values. The gray dots are the raw data points from the 299 sampled plots. The second column contains AUC values for each of the eight regression models across five thresholds of burn severity (**D**, **E**, **F**, **J**, **K**, **L**). Thresholds were created as dichotomization thresholds to produce ROC curves. Overall AUC values represent overall average across five thresholds

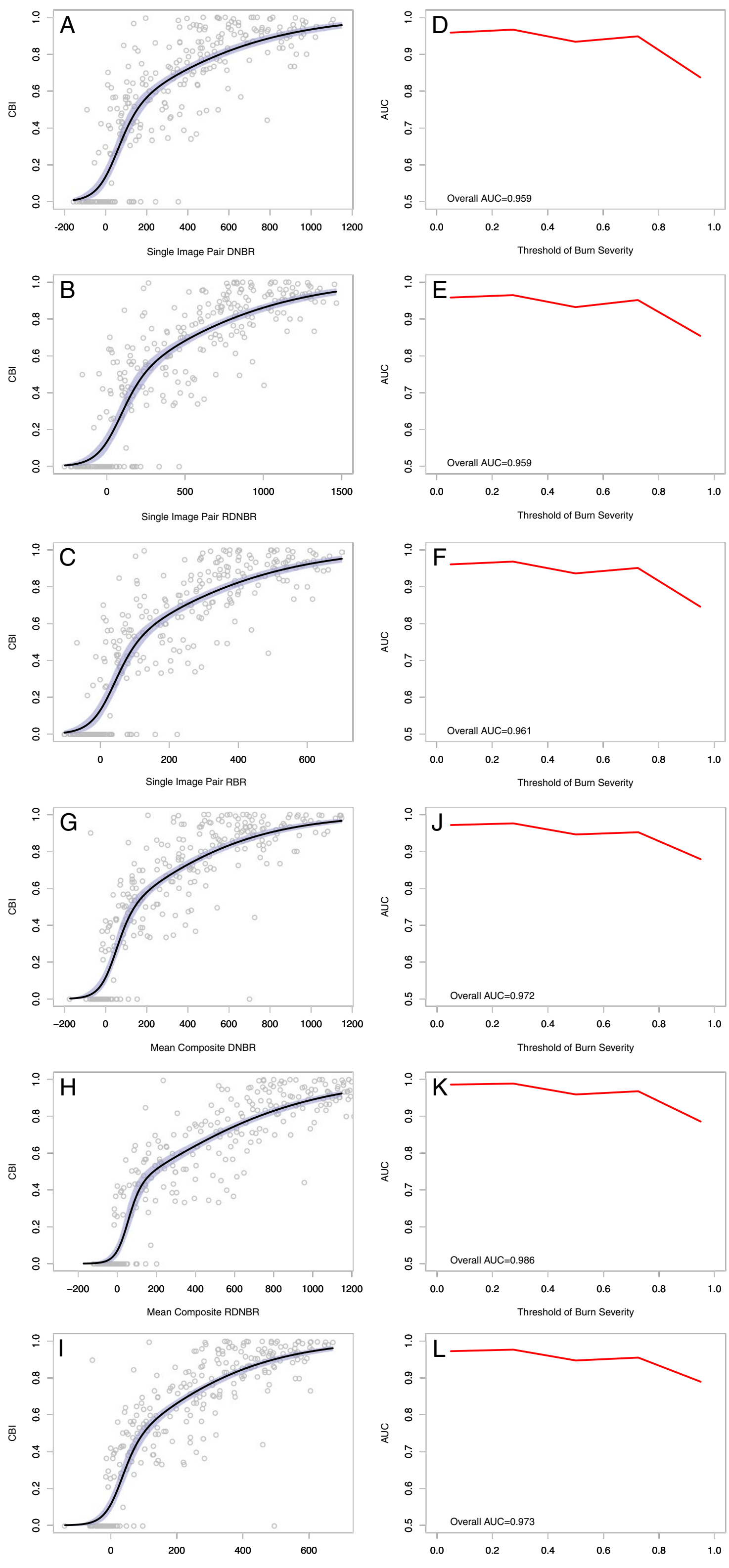

Fig. 3 (See legend on previous page.)

thresholds (Fig. 5D, F, H, J, and Tables S12, S13). Similar to CBI, the relationship between RdNBR and deep char in short-interval reburns was not significant (Q3, Fig. 3O, Table S13).

Discussion

By testing the relationship between widely used field and satellite indices of burn severity in short-interval reburns, our study highlights several key insights for understanding fire effects in reburned landscapes. First, the meaning of CBI and RdNBR in short-interval reburns differs relative to their calibrated values in single fires, but differences depend on the severity of the preceding fire. When short-interval reburns occur where preceding fires were stand-replacing, both indices underestimate metrics of tree canopy burn severity, likely because reburned forests are in an early-seral stage that is more sensitive to fire (Donato et al. 2009a, Donato et al. 2016, Turner et al. 2019). In contrast, when short-interval reburns occur following preceding fires that were not stand-replacing (i.e., low severity), both indices performed consistently well, with one exception being an overestimation of surface burn severity. This outcome is likely because preceding low-severity fires do not strongly alter forest structure but do stimulate understory vegetation response. Second, neither CBI nor RdNBR corresponded to deep charring of woody material in short-interval reburns, which has become commonly observed in reburns and other situations where fire follows soon after other disturbances. This suggests that both indices may be missing an emergent ecological dimension of changing fire regimes that can be explored in future work. Collectively, these findings suggest that burn severity metrics calibrated for single fires provide valuable information in short-interval reburns but their relationship with on-the-ground fire effects can depend on the severity of preceding fires.

Estimation of burn severity in short-interval reburns depends on severity of preceding fire

The underestimation of burn severity in short-interval reburns by CBI and RdNBR when the preceding fire was stand-replacing is likely due to several factors related to the stage of forest recovery at the time of the second fire. Burn severity metrics that were most underestimated in these cases were all related to tree canopy effects: canopy cover, tree mortality, needle and branch retention, and char height. This underestimation is likely due to the magnitude of initial fire-caused change to forest structure by stand-replacing fires, as well as the corresponding fire adaptations common in stand-replacing fire regimes. First, stand replacing fires are a hard reset of successional and stand development dynamics, where any potential fire-resisting traits (e.g., thick bark and high tree crowns) are lost temporarily as young post-fire forests recover over time (Donato et al. 2009a). For species that can develop such fire adaptive traits, it may require many decades after a stand-replacing fire before trees are again able to resist fire, and recovery times vary based on abundance of fire-related traits in the ecosystem (Hood et al. 2018; Stevens et al. 2020). Severe fires regularly occur in forests where trees have adaptations to reproduce following fire (rather than survive fire), such as via canopy seedbanks with species like lodgepole pine (Tinker et al. 1994). However, in early seral stages characterized by young, small, and high-density lodgepole pine trees (e.g., Turner et al. 2016), the tree canopy strata are more vulnerable to fire than an older stand with larger and sparser trees (Kashian et al. 2005) that have a better chance of surviving fire (Stevens et al. 2020). Collectively, the structural condition and lack of fire-resisting traits in forests in an early state of recovery from a recent stand-replacing fire can lead to greater fire severity when the young tree canopy strata is highly fire-sensitive (Donato et al. 2009a, Turner et al. 2019), and our findings demonstrate that field and remote-sensing indices of burn severity correspondingly underestimate these effects.

In contrast to the above context, when short-interval reburns follow preceding low-severity fires, our findings demonstrate that interpretations of CBI and RdNBR are more comparable to their widely used interpretation for single fires. This outcome is likely from the effects of preceding low-severity fires on stand structure (which are modest compared to preceding stand-replacing fires) and the ecological contexts and fire regimes where low-severity fires are more common. Low-severity fires that are not stand-replacing, by definition, leave behind live legacy trees. Therefore, the live forest structure that the second fire encounters is relatively similar to the forest structure of the first fire, suggesting that burn severity indices should perform similarly for tree canopy measures in both fires. Low severity fires are more likely to occur in frequent-fire regimes where trees have fire-resisting traits to survive fire (e.g., thick bark), and understory

(See figure on next page.)

Fig. 4 Zero/one inflated beta regression models eight field measures as the response variable and RdNBR (calculated using GEE method) as the respective predictive variables. In the first column, the black line shows predicted response values (**A**, **C**, **E**, **F**, **I**, **K**, **M**, **O**). The blue polygon around the line shows 95% confidence around mean predicted values. The gray dots are the raw data points from the 299 sampled plots. The second column contains AUC values for each of the eight regression models across five thresholds of burn severity (which were created as dichotomization thresholds to produce ROC curves). Overall AUC values represent overall average across five thresholds (**B**, **D**, **F**, **H**, **J**, **L**, **N**)

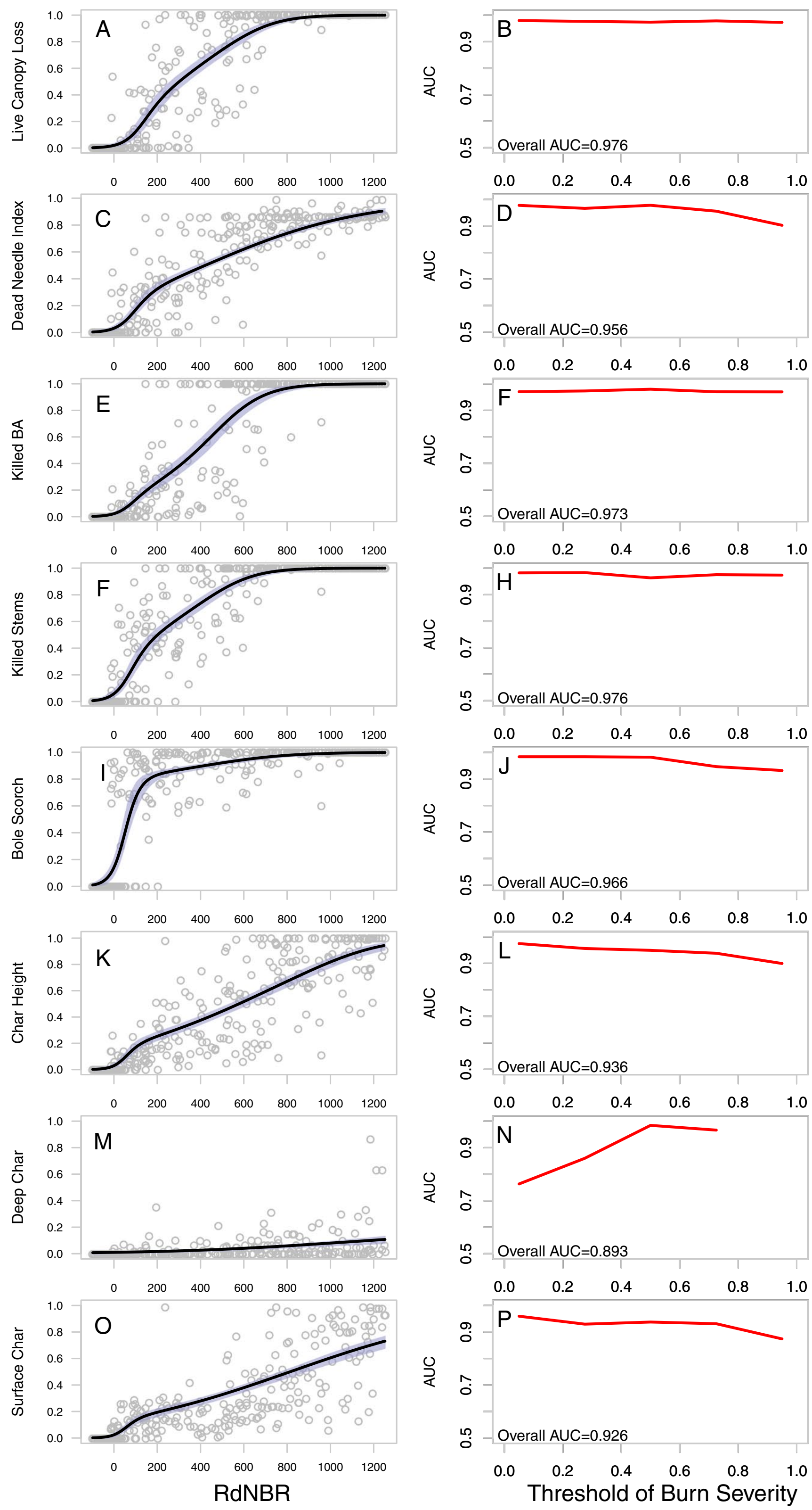

Fig. 4 (See legend on previous page.)

vegetation can recover quickly via re-sprouting (Stevens et al. 2020)—furthering the likelihood of similar conditions encountered by successive fires occurring as a short-interval reburn.

One exception to indices performing similarly to single fires when short-interval reburns follow preceding low-severity fires is that CBI and RdNBR both overestimated surface burn severity in reburns. This may be because non-stand replacing fires are more likely to occur in fire regimes with sparse canopy cover and more vigorous ground cover vegetation, such as in dry forests and woodlands (Hood et al. 2021, Reilly et al. 2021). For example, in ponderosa pine forests or woodlands, frequent surface fires lead to widely spaced and fire-resistant trees interspersed with grasses/herbaceous between large canopy gaps (Agee 1996). Plots with high understory vegetation cover pre-fire are likely to have greater capacity for high understory cover vegetation post-fire, although there is high variability in post-fire vegetation response for low severity burns (Lentile et al. 2007). Therefore, such areas are likely to have resprouting vegetation that obscures post-fire surface charring (the measure overestimated by CBI and RdNBR in such conditions). As CBI and RdNBR indices are measured one-year post fire, this capacity for post-fire understory vegetation recovery may obscure surface burn severity that remains exposed longer post-fire in more closed-canopy forests. This is especially relevant for RdNBR, as spectral indices of surface charring can be less visible from a satellite if vegetative resprouting obscures the forest floor. Fire can influence phenology dates detected via satellites (Peckham et al. 2008), and in systems with vigorous understory vegetation, post-fire green up can occur relatively soon after fire and add to obscuration of char on the forest floor.

Challenges with detecting extreme burn severity and deep charring

Our findings have important implications for the limitations for CBI and RdNBR in detecting deep charring of woody material—one outcome related to extreme levels of burn severity commonly associated with overlapping disturbances. Stand-replacing fires, by killing most or all of trees that are live at the time of fire, produce large numbers of snags and downed logs. In a subsequent fire, much of this woody material can be consumed and integrated into black carbon on the forest floor (e.g., Turner et al. 2019) and/or remain as fragmented logs or snags (Donato et al. 2009b) coated with deep char (Fig. 1, bottom right panel). Conversion of snag biomass to deeply charred material alters the fundamental structure and function of post-fire landscapes (Talucci and Krawchuk 2019; Donato et al. 2016; Campbell et al. 2007), post-fire structural legacies (Harvey et al. 2014; Talucci and Krawchuk 2019), and biogeochemical cycling (Talucci and Krawchuk 2019; Harmon 2001). Other dimensions of severe fire effects, such as soil burn severity (e.g., surface char), are better captured by CBI and RdNBR, and are important for identifying erosion risk and soil hydrophobicity (Robichaud et al. 2007). However, deep char production on standing snags can be decoupled from soil burn severity due to being aerial in nature until snags eventually fall.

The lack of relationship between CBI and deep char in short-interval reburns could be addressed by better integration of deep char into different strata of the protocol. CBI includes deep char as a component in one out of five forest strata (substrate, or forest floor), and therefore does not capture deep char that may occur along boles of live trees or snags that remain standing (Saberi et al. 2022). Augmenting CBI to be able to detect deep char on standing snags separately from charred material on the forest floor can better characterize changes to ecosystem function occurring in short-interval reburns, and is an important area of future research.

The lack of relationship between deep char and RdNBR in short-interval reburns was likely due to limitations from the nature and angle of spectral satellite sensors. The ability of spectral remote sensing to distinguish between deeply charred material and woody material that was only killed by fire is currently not well known. Spectroscopy of pine bark and wood shows differences in the unique spectral signatures for woody material that was burned and/or heated for different lengths of time, which relates to different levels of charred wood (Reeves et al. 2008). However, the spectral similarities between charred and deeply charred woody materials limit the development and/or calibration of bands that can distinguish between the two (Reeves et al. 2008). Thus, the spectral bands used in NBR may not distinguish deeply charred material on pre-fire snags from lighter charred trees that were killed by fire.

(See figure on next page.)

Fig. 5 Zero/one inflated beta regression models for each of the eight individual burn severity metrics with RdNBR (mean composite method) as the predictor variable. In the first column, the no reburn shows model prediction values for non-reburns, while the reburn (1st fire not stand replacing) represents reburns where the first fire was non-stand replacing and the reburn (1st fire stand replacing) represents reburns where the first fire was stand replacing (**A**, **C**, **E**, **G**, **I**, **K**, **M**, **O**, **Q**). The polygon around each line shows 95% confidence around mean predicted values from bootstrapping. Gray dots are the raw data points from the 299 sampled plots. The second column contains AUC values for each of the eight regression models across five thresholds of burn severity (which were created as dichotomization thresholds to produce ROC curves). Overall AUC values represent overall average across five thresholds (**B**, **D**, **F**, **H**, **J**, **L**, **N**, **P**, **R**)

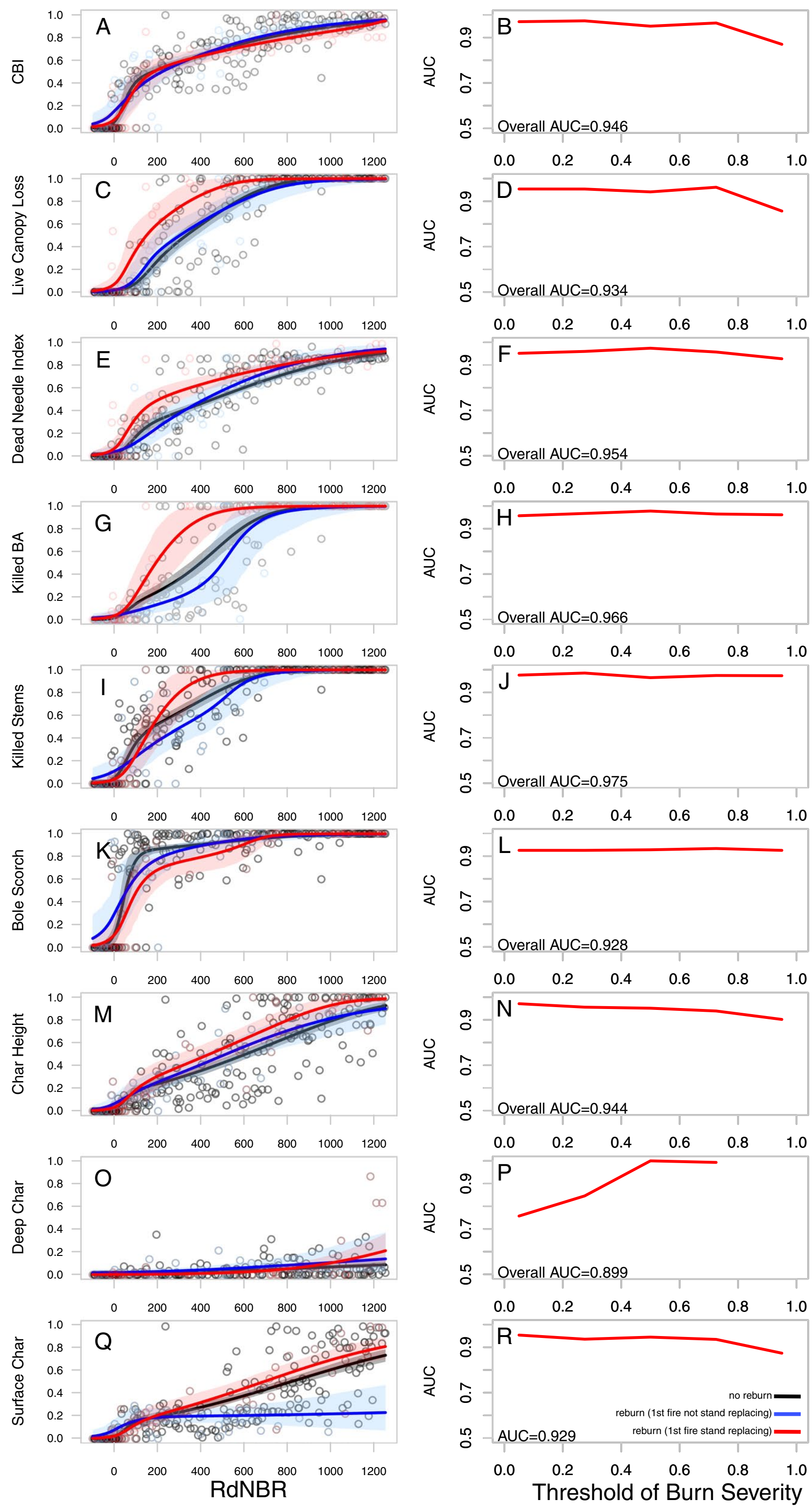

Fig. 5 (See legend on previous page.)

The 2-dimensional top-down perspective of satellite imagery also likely contributes to the poor relationship, as deep charring along the bole of standing snags is a very small proportion of the field of view for the sensor. Most reflectance values change with changes in the view angle for land surfaces (such as forests) that have three-dimensional characteristics (Liang et al. 2000), but Landsat 8 hardcodes the view zenith angle to "0," or directly overhead (Vermote et al. 2016). Multi-angular observations may improve reflectance information retrieval (Schlerf and Atzberger 2012), and incorporation of different or multiple viewing angles could produce different reflectance values that detect deep char on tree surface. Using different or multiple viewing angles from the Landsat Collection 1 Angle Coefficient file (http://www.usgs.gov) to develop stronger relationships with deep char or combining spectral indices like RdNBR with remotely sensed structural indices (e.g., LiDAR) could be explored in future research.

Implications for ecological study of short-interval reburns

Our findings have several important implications for the ecological study of short-interval reburns, which have become an area of heightened research focus in recent decades (Prichard et al. 2017). First, when applying standard satellite remote sensing indices of burn severity to reburns, interpretations of index meanings are different in short-interval reburns than in fires that are occurring after much longer fire-free periods. Studies using satellite indices to test the effects of prior fires on burn severity in subsequent reburns have generally found that very short intervals between fires are characterized by negative feedbacks indicated from lower severity in the second fire (e.g., Parks et al. 2014a,b, Harvey et al. 2016a, Cansler et al. 2022). However, our findings suggest that when the first fire is stand-replacing, severity in a subsequent reburn can be greater than satellite indices suggest, as the same level of RdNBR represents more severe fire effects for several measures. As such, negative feedbacks between fires over short intervals may be weaker than suggested by analyses that assume RdNBR means the same thing in both fires. Conversely, when the first fire is low severity/non-stand-replacing, our findings suggest that this outcome is flipped for forest floor measures, in that negative feedbacks between fires over short intervals may be stronger than suggested by assuming that RdNBR means the same thing in both fires.

A second implication for ecological study of reburns is that standard field measures and satellite indices of burn severity are likely under-detecting key dimensions of extreme burn severity that has been documented in recent short-interval reburns when both fires are severe. CBI and RdNBR were designed primarily outside the context of successive stand-replacing fires (where they both perform very reliably), though such conditions are increasingly characterized by high-levels of coarse wood consumption (Donato et al. 2009a,b, Turner et al. 2019), charred snag production (Harvey et al. 2014, Talluci and Krawchuk 2019), and compound disturbance effects from removal of key biological legacies (Johnstone et al. 2016). As such, the magnitude and spatial extent of extreme burn severity and corresponding ecological impacts may be underestimated now and in the future until there are better ways to incorporate them into these or other indices.

Conclusion

As fire activity increases and more areas burn multiple times in short succession, accurate monitoring and assessment of (re)burn severity becomes more important. Overall, our models show that both CBI and RdNBR relate to burn severity similarly for some measures, and diverge for others, between areas that have burned once vs. twice in recent decades. In general, our results suggest that these widely used indices of burn severity may be under-predicting canopy burn severity in short-interval reburns where the preceding fire was stand-replacing, and over-predicting surface burn severity in short-interval reburns where the preceding fire was non-stand-replacing. Furthermore, neither index corresponded to deep charring of woody material, suggesting that this important aspect of extreme burn severity that can occur in short-interval reburns may not be well captured by burn severity mapping efforts. These findings can help qualitatively inform where burn severity in short-interval reburns is being under- or over-estimated and can guide development of better quantitative adjustments to improve burn severity assessments in the future.

Supplementary Information

The online version contains supplementary material available at https://doi.org/10.1186/s42408-023-00178-3.

Additional file 1: Table S1. AUC values for CBI-based reburn models at five classification thresholds. **Table S2.** Model outputs showing estimate, standard error, and p-value for mu, nu, and tau parameters for eight models with each individual field metric as a function of CBI. Non-SR = non-stand replacing, SR= stand replacing. **Table S3.** Individual AUC values for each satellite index-based model (composite method) across five burn severity classification thresholds. **Table S4.** Outputs showing estimate, standard error, and p-value for three models for mu, nu, and tau parameters with CBI as a function of each spectral index. Note NBRs are calculated with the composite method. **Table S5.** Fires and associated satellite imagery data for the single-image method. **Table S6.** Individual AUC values for each satellite index-based model across five burn severity classification thresholds. Shows dNBR, RdNBR, and RBR to all have around a 96% accuracy in classifying burn severity at five distinct classification thresholds, suggesting the indices are nearly identical in their relationship to CBI. **Table S7.** Outputs showing estimate, standard error, and p-value for three models for mu, nu, and tau parameters with CBI as a function of each spectral index. **Figure S1.** Zero/one inflated beta regression models eight field measures as the response variable and RdNBR (calculated using the single image method) as the respective predictive variables. In the first column, the black line shows predicted response values (A,C,E,G,I,K,M,O). The blue polygon around the line shows 95% confidence around mean predicted values. The grey dots are the raw data points from the 315 sampled plots. The second column contains AUC values for each of the eight regression models across five thresholds of burn severity (which were created as dichotomization thresholds to produce ROC curves). Overall AUC values represent overall average across five thresholds (B,D,F,H,J,L,N,P). **Table S8.** AUC values for RdNBR-based, non-reburn models at five classification thresholds. **Table S9.** Outputs showing estimate, standard error, and p-value for each of the individual field measure models for mu, nu, and tau parameters as a function of RdNBR (calculated with single image method). **Table S10.** AUC values for RdNBR-models at five classification thresholds (GEE). **Table S11.** Outputs showing estimate, standard error, and p-value for each of the individual field measure models for mu, nu, and tau parameters as a function of RdNBR (calculated with GEE method). **Table S12.** AUC values for RdNBR-based reburn models at five classification thresholds (GEE). **Table S13.** Model outputs showing estimate, standard error, and p-value for mu, nu, and tau parameters for nine models with each individual field metric as a function of RdNBR. Non SR = non-stand replacing, SR= stand replacing.

Acknowledgements
We thank C Baker and the USFS Geospatial Technology Applications Center for technical and logistical support. We thank S. Salam, E. Pletcher, L. Walden, P. Hauschka, C. Zender, J. Weatherholt, and M. Agne for their invaluable help in the field. We thank E. Alvarado and D. Butman, MG Turner, and JE Morris for insightful discussions and constructive feedback about this project. We thank MS Buonanduci for statistical advice and we thank NP Young for inspiration for the title of the paper. We thank R Keane and three anonymous reviewers for comments that improved the manuscript. We thank M. Dillon and the University of Wyoming-National Park Service Research Station staff for logistical support and Yellowstone NP, Grand Teton NP, and the US Forest Service for facilitating this study under research permits specific to each field location.

Authors' contributions
BJ Harvey conceived of the study and acquired funding. SJ Saberi collected and analyzed the data with input from BJ Harvey. SJ Saberi and BJ Harvey wrote the manuscript. Both authors read and approved the final manuscript.

Funding
This project was funded by NSF Grant DEB-1719905 and USDA Agreement 17-CS-11130400-010 awarded to BJ Harvey. BJ Harvey acknowledges additional support from the University of Washington School of Environmental and Forest Sciences and from the Jack Corkery and George Corkery Jr. Endowed Professorship in Forest Sciences. SJ Saberi acknowledges support from the Graduation Opportunities and Minorities Achievement Program and the School of Environmental and Forest Sciences while completing her degree at the University of Washington.

Availability of data and materials
The datasets generated and/or analyzed during the current study are available in the author's Zenodo repository.

Declarations

Ethics approval and consent to participate
Not applicable.

Consent for publication
Not applicable.

Competing interests
The authors declare that they have no competing interests.

Received: 16 May 2022 Accepted: 8 March 2023
Published online: 20 April 2023

References
Agee, J. K. 1996. *Fire Ecology of Pacific Northwest forests*. Island Press, Washington D.C.

Bird, M. I., J. G. Wynn, G. Saiz, C. M. Wurster, and A. McBeath. 2015. The pyrogenic carbon cycle. *Annual Review of Earth and Planetary Sciences* 43: 273–298. https://doi.org/10.1146/annurev-earth-060614-105038.

Bradbury, S. M. 2006. Response of the post-fire bryophyte community to salvage logging in boreal mixed wood forests of northeastern Alberta, Canada. *Forest Ecology and Management* 234: 313–322. https://doi.org/10.1016/j.foreco.2006.07.013.

Campbell, J., D. Donato, D. Azuma, and B. Law. 2007. Pyrogenic carbon emission from a large wildfire in Oregon, United States. *Journal of Geophysical Research: Biogeosciences* G4:112. https://doi.org/10.1029/2007JG000451.

Cansler, C. A., and D. McKenzie. 2012. How robust are burn severity indices when applied in a new region? Evaluation of alternate field-based and remote-sensing methods. *Remote sensing* 4: 456–483. https://doi.org/10.3390/rs4020456.

Cansler, C. A., V.R. Kane, P.F. Hessburg, J.T. Kane, S.M.A. Jeronimo, J.A. Lutz, N.A. Povack, D.J. Churchill, and A.J. Larson. 2022. Previous wildfires and management treatments moderate subsequent fire severity. *Forest Ecology and Management* 50: 119764. https://doi.org/10.1016/j.foreco.2021.119764.

Czimczik, C. I., C. M. Preston, M. W. I. Schmidt, R. A. Werner, and E. D. Schulze. 2002. Effects of charring on mass, organic carbon, and stable carbon isotope composition of wood. *Organic Geochemistry* 33: 1207–1223. https://doi.org/10.1016/S0146-6380(02)00137-7.

Donato, D. C., J. L. Campbell, J. B. Fontaine, and B. E. Law. 2009b. Quantifying char in postfire woody detritus inventories. *Fire Ecology* 5: 104–115. https://doi.org/10.4996/fireecology.0502104.

Donato, D.. C., J.. B. Fontaine, W.. D. Robinson, J.. B. Kauffman, and B.. E. Law. 2009a. Vegetation response to a short interval between high-severity wildfires in a mixed-evergreen forest. *Journal of Ecology* 97: 142–154. https://doi.org/10.1111/j.1365-2745.2008.01456.x.

Donato, D. C., J. B. Fontaine, and J. L. Campbell. 2016. Burning the legacy? Influence of wildfire reburn on dead wood dynamics in a temperate conifer forest. Ecosphere 7: e01341. https://esajournals.onlinelibrary.wiley.com/doi/abs/https://doi.org/10.1002/ecs2.1341.

Enright, N. J., J. B. Fontaine, D. M. Bowman, R. A. Bradstock, and R. J. Williams. 2015. Interval squeeze: altered fire regimes and demographic responses interact to threaten woody species persistence as climate changes. *Frontiers in Ecology and the Environment* 13: 265–272. https://doi.org/10.1890/140231.

Harmon, M. E. 2001. Moving towards a new paradigm for Woody Detritus Management. Ecological Bulletins 49: 269–278. https://www.jstor.org/stable/20113283.

Harvey, B.. J., D.. C. Donato, and M.. G. Turner. 2014. Recent mountain pine beetle outbreaks, wildfire severity, and postfire tree regeneration in the US Northern Rockies. *Proceedings of the National Academy of Sciences* 111: 15120–15125.

Harvey, B. J., D. C. Donato, and M. G. Turner. 2016a. Burn me twice, shame on who? Interactions between successive forest fires across a temperate mountain region. *Ecology* 97: 2272–2282.

Harvey, B. J., D. C. Donato, and M. G. Turner. 2016b. Drivers and trends in landscape patterns of stand-replacing fire in forests of the US Northern Rocky Mountains (1984–2010). *Landscape Ecology* 31: 2367–2383.

Harvey, B. J., R. A. Andrus, and S. C. Anderson. 2019. Incorporating biophysical gradients and uncertainty into burn severity maps in a temperate fire-prone forested region. *Ecosphere* 10: e02600.

Hood, M., Harvey J. Sharon, Fornwalt J. Brian, Naficy E. Paula, D. Cameron, Hanson, Davis T. Winslow, Battaglia A. Kimberly, and S. Mike, Stevens-Rumann Camille, and Victoria Ann Saab. 2021. Fire Ecology of Rocky Mountain Forests. Fire Ecology and Management: Past Present, and Future of US Forested Ecosystems eds. Cathryn H. Greenberg and Beverly Collins 39:287–336. Springer, Cham, Switzerland. https://doi.org/10.1007/978-3-030-73267-7_8.

Hood, S. M., J. M. Varner, P. Van Mantgem, and C. A. Cansler. 2018. Fire and tree death: understanding and improving modeling of fire-induced tree mortality. *Environmental Research Letters* 13: 113004.

Huang, Y., Y. Jin, M. W. Schwartz, and J. H. Thorne. 2020. Intensified burn severity in California's northern coastal mountains by drier climatic condition. *Environmental Research Letters* 15: 104033. https://doi.org/10.1088/1748-9326/aba6af.

Johnstone, J. F., C.D. Allen, J.F. Franklin, L.E. Frelich, B.J. Harvey, P.E. Higuera, M.C. Mack, R.K. Meentemeyer, M.R. Metz, G.W.L. Perry, T. Schoennagel, and M.G. Turner. 2016. Changing disturbance regimes, ecological memory, and forest resilience. *Frontiers in Ecology and the Environment* 14: 369-378. https://doi.org/10.1002/fee.1311.

Kashian, D. M., M. G. Turner, W. H. Romme, and C. G. Lorimer. 2005. Variability and convergence in stand structural development on a fire-dominated subalpine landscape. *Ecology* 86: 643–654.

Keeley, J. E. 2009. Fire intensity, fire severity and burn severity: a brief review and suggested usage. *International Journal of Wildland Fire* 18: 116–126.

Key, C. H., and N. C. Benson. 2006. Landscape Assessment in FIREMON: Fire effects monitoring and inventory system. LA1-55. General technical report RMRS-GTR-164-CD.https://doi.org/10.2737/RMRS-GTR-164.

Konkathi, P., and A. Shetty. 2021. Inter comparison of post-fire burn severity indices of Landsat-8 and Sentinel-2 imagery using Google Earth Engine. *Earth Science Informatics* 14: 645–653. https://doi.org/10.1007/s12145-020-00566-2.

Larson, A. J., R. T. Belote, C. A. Cansler, S. A. Parks, and M. S. Dietz. 2013. Latent resilience in ponderosa pine forest: effects of resumed frequent fire. *Ecological Applications* 23: 1243–1249.

Lentile, L. B., P. Morgan, A. T. Hudak, M. J. Bobbitt, S. A. Lewis, A. M. S. Smith, and P. R. Robichaud. 2007. Post-Fire burn severity and vegetation response following eight large wildfires across the Western United States. *Fire Ecology* 3: 91–108.

Liang, S., A. H. Strahler, M. J. Barnsley, C. C. Borel, S. A. W. Gerstl, D. J. Diner, A. J. Prata, and C. L. Walthall. 2000. Multiangle remote sensing: past, present and future. *Remote Sensing Reviews* 18: 83–102.

Lutz, J. A., C. H. Key, C. A. Kolden, J. T. Kane, and J. W. Van Wagtendonk. 2011. Fire frequency, area burned, and severity: a quantitative approach to defining a normal fire year. *Fire Ecology* 7: 51–65. https://doi.org/10.4996/fireecology.0702051.

Marañón-Jiménez, S., J. Castro, E. Fernández-Ondoño, and R. Zamora. 2013. Charred wood remaining after a wildfire as a reservoir of macro- and micronutrients in a Mediterranean pine forest. *International Journal of Wildland Fire* 22: 681–695. https://doi.org/10.1071/WF12030.

Miller, J. D., and A. E. Thode. 2007. Quantifying burn severity in a heterogenous landscape with a relative version of the delta normalized burn ratio (dNBR). *Remote Sensing of Environment* 109: 66–80.

Miller, J. D., E. E. Knapp, C. H. Key, C. N. Skinner, C. J. Isbell, R. M. Creasy, and J. W. Sherlock. 2009. Calibration and validation of the relative differenced normalized burn ratio (RdNBR) to three measures of fire severity in the Sierra Nevada and Klamath Mountains, California, USA. *Remote Sensing of Environment* 113: 645–656.

Morgan, P., R. E. Keane, G. K. Dillon, T. B. Jain, A. T. Hudak, E. C. Karau, P. G. Sikkink, Z. E. Holden, and E. K. Strand. 2014. Challenges of assessing fire and burn severity using field measures, remote sensing and modelling. *International Journal of Wildland Fire* 23: 1045–1060.

Muff, S., E. B. Nilsen, R. B. O'Hara, and C. R. Nater. 2022. Rewriting results sections in the language of evidence. *Trends in Ecology & Evolution* 37: 203–210.

Parks, S. A., C. Miller, C. R. Nelson, and Z. A. Holden. 2014a. Previous fires moderate burn severity of subsequent wildland fires in two large western US wilderness areas. *Ecosystems* 17: 29–42.

Parks, S. A., G. K. Dillon, and C. Miller. 2014b. A new metric for quantifying burn severity: the Relativized burn ratio. *Remote Sensing* 6 (3): 1827–1844. https://doi.org/10.3390/rs6031827.

Parks, S. A., L. M. Holsinger, C. Miller, and C. R. Nelson. 2015. Wildland fire as a self-regulating mechanism: the role of previous burns and weather in limiting fire progression. *Ecological Applications* 25: 1478–1492.

Parks, S. A., L. M. Holsinger, M. A. Voss, R. A. Loehman, and N. P. Robinson. 2018. Mean composite fire severity computed with Google Earth Engine offer improved accuracy and expanded mapping potential. *Remote Sensing* 10 (6): 879. https://doi.org/10.3390/rs10060879.

Pearce, J. and S. Ferrier. 2000. Evaluating the predictive performance of habitat models developed using logistic regression. *Ecological modelling* 133: 225-245. https://doi.org/10.1016/S0304-3800(00)00322-7.

Peckham, S. D., D. E. Ahl, S. P. Serbin, and S. T. Gower. 2008. Fire-induced changes in green-up and leaf maturity of the canadian boreal forest. *Remote Sensing of Environment* 112: 3594–3603.

Picotte, J. J., and K. M. Robertson. 2011. Validation of remote sensing of burn severity in south-eastern US ecosystems. *International Journal of Wildland Fire* 20: 453–464. https://doi.org/10.1071/WF10013.

Povak, N. A., V. R. Kane, B. M. Collins, J. M. Lydersen, J.T. and Kane. 2020. Multi-scaled drivers of severity patterns vary across land ownerships for the 2013 Rim Fire, California. *Landscape Ecology* 35: 293–318. https://doi.org/10.1007/s10980-019-00947-z.

Prichard, S. J., C. S. Stevens-Rumann, and P. F. Hessburg. 2017. Tamm Review: shifting global fire regimes: Lessons from reburns and research needs. *Forest Ecology and Management* 396: 217–233.

Pyne, S. J., P. L. Andrews, and R. D. Laven. 1996. Introduction to wildland fire, Second edition. New York, USA: Wiley.

Ramsey, F., and D. Schafer. 2012. The statistical sleuth: a course in methods of data analysis. *Cengage Learning*.

Reeves, J. B., G. W. McCarty, D. W. Rutherford, and R. L. Wershaw. 2008. Mid-infrared diffuse Reflectance Spectroscopic examination of Charred Pine Wood, Bark, Cellulose, and lignin: implications for the quantitative determination of Charcoal in Soils. *Applied Spectroscopy* 62: 182–189.

Rielly, J., Halofsky E. Matthew, Krawchuk A. Jessica, Donato C. Meg, F. Daniel,Hessburg, Johnston D. Paul, Merschel G. James, Swanson E. Andrew, Halofsky S. Mark, Joshua, and Spies A. Thomas. 2021. Fire Ecology and Management in Pacific Northwest forests. In *Fire Ecology and Management: Past Present, and future of US Forested Ecosystems eds. Cathryn H. Greenberg and Beverly Collins*, 393–436. Cham, Switzerland: Springer.

Robichaud, P. R., S. A. Lewis, D. Y. M. Laes, A. T. Hudak, R. F. Kokaly, and J. A. Zamudio. 2007. Postfire soil burn severity mapping with hyperspectral image unmixing. *Remote Sensing of Environment* 108: 467–480. https://doi.org/10.1016/j.rse.2006.11.027.

Saberi, S. J. 2019. *Quantifying burn severity in forests of the interior Pacific Northwest: From field measurements to satellite spectral indices*. Master's thesis, University of Washington, Seattle. UW Research Works Archive. https://digital.lib.washington.edu/researchworks/handle/1773/45201.

Saberi, S. J., M. C. Agne, and B. J. Harvey. 2022. Do you CBI what I see? The relationship between the composite burn Index and quantitative field measures of burn severity varies across gradients of forest structure. *International Journal of Wildland Fire* 31 (2): 112–123. https://doi.org/10.1071/WF21062.

Schlerf, M., and C. Atzberger. 2012. Vegetation structure Retrieval in Beech and Spruce forests using Spectrodirectional Satellite Data. *IEEE Journal of Selected Topics in Applied Earth Observations and Remote Sensing* 5: 8–17.

Singh, N., S. Abvien, M. S. Torn, and M. W. I. Schmidt. 2012. Fire-derived organic carbon in soil turns over on a centennial scale. *Biogeosciences* 9: 2847–2857. https://doi.org/10.5194/bg-9-2847-2012.

Stevens, J. T., M. M. Kling, D. W. Schwilk, J. M. Varner, and J. M. Kane. 2020. Biogeography of fire regimes in western U.S. conifer forests: a trait-based approach. *Global Ecology and Biogeography* 29: 944–955.

Stevens-Rumann, C. and P. Morgan. 2016. Repeated wildfires alter forest recovery of mixed-conifer ecosystems. *Ecological Applications* 26: 1842-1853. https://doi.org/10.1890/15-1521.1.

Talucci, A. C., and M. A. Krawchuk. 2019. Dead forests burning: the influence of beetle outbreaks on fire severity and legacy structure in sub-boreal forests. *Ecosphere* 10: 5: e02744.

Tinker, D. B., W. H. Romme, W. W. Hargrove, R. H. Gardner, and M. G. Turner. 1994. Landscape-scale heterogeneity in lodgepole pine serotiny. *Canadian Journal of Forest Research* 24: 897–903.

Turner, M. G., T. G. Whitby, D. B. Tinker, and W. H. Romme. 2016. Twenty-four years after the Yellowstone fires: are postfire lodgepole pine stands converging in structure and function? *Ecology* 97: 1260–1273.

Turner, M. G., K. H. Braziunas, W. D. Hansen, and B. J. Harvey. 2019. Short-interval severe fire erodes the resilience of subalpine lodgepole pine forests. *Proceedings of the National Academy of Sciences* 116:11319–11328.
Vermote, E., C. Justice, M. Claverie, and B. Franch. 2016. Preliminary analysis of the performance of the Landsat 8/OLI land surface reflectance product. *Remote Sensing of Environment* 185: 46–56.

Publisher's Note